Formation and dynamics of finite amplitude localized pulses in elastic tubes

B. Eliasson and P. K. Shukla
Institut für Theoretische Physik IV, Ruhr-Universität Bochum, D-44780 Bochum, Germany
(Received 2 March 2005; revised manuscript received 15 April 2005; published 28 June 2005)

We present theoretical and simulation studies of the formation and dynamics of finite-amplitude localized pulses (solitary waves) of an incompressible fluid in an elastic tube. Starting from a set of hydrodynamic equations, we derive a Hamiltonian which represents the energy integral of our system. The energy integral is analyzed to obtain explicit profiles of finite-amplitude solitary pulses. Also studied are the excitation and dynamics of solitary pulses by using computer simulations. It is found that a train of solitary pulses can be excited by the nonlinear self-steepening at shock fronts. The relevance of our investigation to blood solitary waves in arteries is discussed.

DOI: 10.1103/PhysRevE.71.067302 PACS number(s): 47.15.−x, 87.19.Tt, 47.35.+i

I. INTRODUCTION

Measurements of the amplitude and pressure of the blood flow in the ascending aorta of a dog [1] (also in Ref. [2]) and rabbits [3] have shown that the blood flow has a pulselike form, suggesting that the dynamics of the blood flow in arteries may be characterized as solitary waves which keep their pulselike shape due to a balance between the dispersion and nonlinearities of the wave. The blood is described as an incompressible fluid which flows in a thin elastic tube. The basic nonlinear model for the nonlinear propagation of an inelastic fluid in an elastic tube were derived in the 1980s [2,4,5], where the existence of solitary waves was demonstrated by means of solutions to a derived Korteweg–de Vries (KdV) equation. The theory of the blood dynamics has since been developed significantly in the small-amplitude limit [7–11], including interactions between blood solitary waves [12]. Neglecting the dispersive (time derivative) term in Eq. (3) below, simple-wave (monovariable) solutions of the fully nonlinear system were derived for the case of a spatially varying Young's module, demonstrating the pulse steepening and the formation of shocks [6].

In this Brief Report, we analyze the nonlinear equations describing the deformation of an elastic tube filled with a nonelastic and nonviscous fluid, where the radial fluid velocities are assumed to be small compared to axial velocities—a scenario relevant for the blood flow in arteries. First, we show that the nonlinear equations in a stationary frame can be expressed in the form of an energy integral [13,14]. The latter is analyzed to demonstrate the existence and shape of large-amplitude solitary pulses, as well as their dependence on the solitary-wave speed and the value of the nonlinear elasticity coefficient. Second, we perform numerical simulations of the time-dependent nonlinear equations. Our results reveal self-steepening and excitation of large-amplitude solitary pulses.

II. THEORY AND SIMULATIONS

The physics of solitary pulses in an elastic tube is described by a conservation of the fluid and a balance between the inertia of the fluid and the pressure, which are mediated by the elastic properties of the tube wall. For solitary pulses with scale lengths much larger than the tube diameter, a one-dimensional model can be used [12], which neglects the detailed three-dimensional dynamics of the fluid and only considers the mean motion of the fluid along the tube axis. The equations then reduce to a description of the mean fluid velocity in the tube and the elastic perturbation of the tube cross section, where the force is due to the pressure difference between the atmospheric pressure and the pressure inside the tube. The basic one-dimensional equations for describing the dynamics of localized pressure waves in an elastic tube are [2] the continuity equation

$$\frac{\partial A}{\partial t}+\frac{\partial (Av_z)}{\partial z}=0, \tag{1}$$

where A is the cross-section area of the tube and v_z is the axial flow speed of the blood, together with the axial equation of motion of the fluid and the radial equation of motion of the tube wall, respectively,

$$\frac{\partial v_z}{\partial t}+v_z\frac{\partial v_z}{\partial z}=-\frac{1}{\rho}\frac{\partial P}{\partial z} \tag{2}$$

and

$$\rho H\frac{\partial^2 R}{\partial t^2}=(P-P_e)-\frac{h}{R}\sigma_t, \tag{3}$$

where $R=R_0+r$ is the radius of the tube where R_0 is the unperturbed tube radius, P is the pressure inside the tube, P_e is the (atmospheric) pressure outside the tube, ρ is the density, and H and h are the effective inertial thickness and the thickness of the wall, respectively. The tangential stress of the tube wall is represented by

$$\sigma_t=E\frac{r}{R_0}\left(1+a\frac{r}{R_0}\right), \tag{4}$$

where E is Young's module and a is a nonlinear coefficient of elasticity. Using the conditions for the conservation of mass of the wall, $RH=R_0H_0$ and $Rh=R_0h_0$, where R_0, H_0, and h_0 are the equilibrium values of R, H, and h, respectively, and the approximate relation $A=\pi R^2\approx\pi(R_0^2+2R_0r)$,

 ©2005 The American Physical Society

the quantities r, H, and h can be eliminated from Eqs. (1)–(4). The latter can be cast into the dimensionless form as

$$\frac{\partial S}{\partial t}+\frac{\partial (Su)}{\partial x}=0, \tag{5}$$

$$\frac{\partial u}{\partial t}+u\frac{\partial u}{\partial x}=-\frac{\partial p}{\partial x}, \tag{6}$$

and

$$p=\frac{2}{1+S}\frac{\partial^2 S}{\partial t^2}+\frac{2(S-1)[2+\alpha(S-1)]}{(1+S)^2}, \tag{7}$$

where we have normalized the space and time by [2,10] $L_0=(R_0H_0/2)^{1/2}$ and $T_0=(\rho H_0R_0^2/h_0E)^{1/2}$, respectively. Furthermore, we have also normalized the cross section and speed as $S=A/\pi R_0^2$ and $u=v_z/c_0$ where the linear-wave speed is $c_0=L_0/T_0=(h_0E/2\rho R_0)^{1/2}$. The normalized pressure perturbation is $p=(P-P_e)/P_0$, where $P_0=h_0E/2R_0$. For future (numerical) convenience, we note that the time derivative in Eq. (7) can be eliminated with the help of Eqs. (5) and (6), so that the pressure can be written in an alternative form as

$$p-\frac{2}{1+S}\frac{\partial}{\partial x}\left(S\frac{\partial p}{\partial x}\right)=\frac{2}{1+S}\frac{\partial^2 (Su^2)}{\partial x^2}+\frac{2(S-1)[2+\alpha(S-1)]}{(S+1)^2}, \tag{8}$$

which gives p implicitly as a solution of the linear ordinary differential equation with appropriate boundary conditions.

Assuming that all quantities depend only on $\xi=x-v_0t$, we have from Eqs. (5) and (6) $-v_0S+Su=-v_0$ and $-v_0u+u^2/2=-p$, where we have used the boundary conditions $S=1$ and $u=p=0$ at $|\xi|=\infty$. Eliminating u from Eqs. (5) and (6), we have $p=v_0^2(S^2-1)/2S$. The latter is inserted into Eq. (7) to obtain

$$\frac{d^2S}{d\xi^2}+\frac{(S-1)[2+\alpha(S-1)]}{v_0^2(S+1)}-\frac{(S+1)^2(S-1)}{4S^2}=0. \tag{9}$$

Multiplying Eq. (9) by $dS/d\xi$, we can integrate the resultant equation once with respect to ξ to obtain the Hamiltonian

$$H=\frac{1}{2}\left(\frac{dS}{d\xi}\right)^2+\psi(S)=0, \tag{10}$$

where the classical (Sagdeev) potential [13] for our purposes reads

$$\psi(S)=\frac{1}{v_0^2}\left[(2-3\alpha)(S-1)+\frac{\alpha(S^2-1)}{2}+4(\alpha-1)\ln\left(\frac{S+1}{2}\right)\right]-\frac{S^2}{8}-\frac{S}{4}+\frac{5}{8}-\frac{1}{4S}+\frac{\ln S}{4}. \tag{11}$$

Localized solitary pulse solutions are allowed if $\psi=d\psi/dS=0$ at $S=1$ and $\psi=0$ and $d\psi/dS\neq 0$ at $S=S_0>1$; the maximum value of S will then be $S=S_0$ at the peak of the solitary pulse.

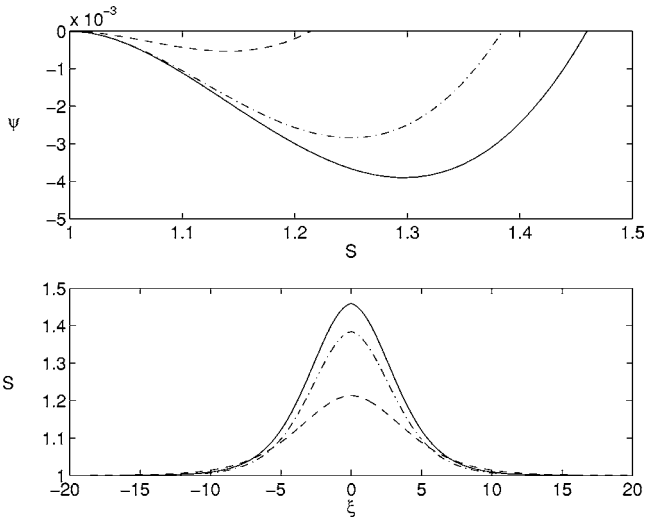

FIG. 1. The Sagdeev potential, describing the amplitude of the blood solitary waves (upper panel), and the corresponding profile of the solitary pulses, for different sets of parameters: $\alpha=2$ and $v_0=1.2$ (solid lines), $\alpha=2$ and $v_0=1.1$ (dashed lines), and $\alpha=2.5$ and $v_0=1.2$ (dash-dotted lines).

In Fig. 1, we have plotted the Sagdeev potential as a function of S (upper panel) and have integrated Eq. (10) numerically with respect to ξ and have plotted the corresponding profiles of the tube cross section (lower panel) of localized pulses. Comparing the amplitudes of the solitary pulses, we notice that larger pulse speeds v_0 support larger-amplitude solitary pulses, while a larger α value leads to a smaller amplitude of the localized pulse. Next, we turn to numerical solutions of the original system of equations (5) and (6), and where the pressure was obtained from Eq. (8). The x derivatives in Eqs. (5), (6), and (8) are approximated with difference approximations and the resulting linear equation system in Eq. (8) is solved numerically as a boundary value problem, where the value of p is set to zero at the boundaries far away from the pulse. The solution is advanced in time with a fourth-order Runge-Kutta method. First, the initial condition is taken to be a Gaussian pulse of the form $S=1+0.3\exp[-(x+300)^2/900]$ and the velocity is initially set to $u=1.2(1-1/S)$. The nonlinear parameter was $\alpha=2.0$ in the simulation. The numerical results are displayed in Fig. 2 for the tube cross section (upper panels) and velocity (lower panels). We see that the initial pulse first self-steepens and creates a shocklike structure at $t=120$. At later times, the shock front begins to break up into oscillations, and the amplitudes of localized pulses increase. At $t=480$, we see that a few large-amplitude solitary pulses have been created; the amplitude of the largest solitary pulse is approximately twice the one of the initial pulse. We note that the largest-amplitude localized pulse propagates with the highest speed, which is in agreement with our theoretical result in Fig. 1. In the experimental observations of the flow velocity and pressure at five points in the ascending aorta to the saphenous artery in a dog [1,2], one sees the increase of the amplitude and decrease of the width of a pressure pulse, and the formation of dicrotic (twice beating) pulses. The measured parameters for the thoracic aorta were $R_0=0.5$ cm,

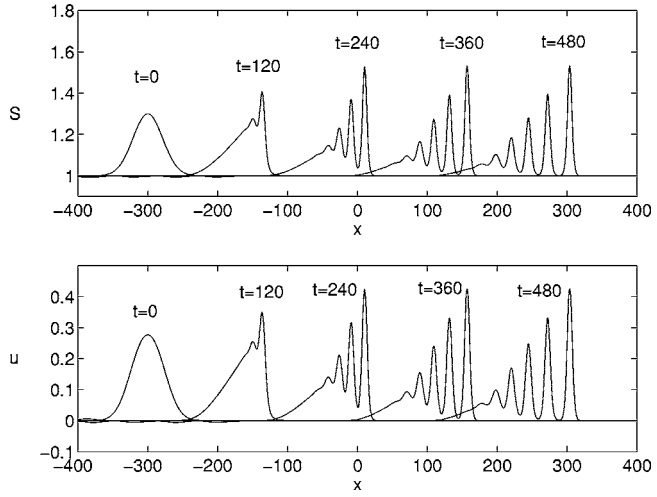

FIG. 2. The profile of the tube cross section S (upper panel) and velocity u (lower panel) at different times, for $\alpha=2.0$.

$h_0/r_0=0.12$, and $\rho\approx 1$ g/cm^2. By comparing the static model with measurements of the dependence of the pressure on the radius in the thoracic aorta of a dog (presented by McDonald [1]), Yomosa [2] estimated Young's module to 5.37×10^6 dyn/cm^2 and the nonlinear coefficient of elasticity to $\alpha=1.95$ for this case. The amplitude of the measured initial pressure pulse was 20 mm Hg, which in our scaled units corresponds to a pressure with the amplitude $p_{\max}\approx 0.1$. In order to compare with the experiment, we have performed a simulation where we initially have a pulse train of the form $S=1+0.025\{1-\tanh[-5\cos(2\times 10^{-3}\pi x)+2.5]\}\times[1+\sin(2\pi x/50)]$ and $u=1.1(1-1/S)$; see the upper panels of Fig. 3, where we have displayed the initial profiles of the velocity and pressure. We see that the initially modulated harmonic wave self-steepens and increases its amplitude as time advances. In the lower panels (for $t=132$ and $t=198$), we see the formation of narrow dicrotic pulses similar to the pressure pulses observed in the experiment [1,2].

III. SUMMARY

To summarize, we have presented an investigation of the formation and dynamics of large-amplitude solitary pulses of an incompressible and inviscid fluid in an elastic tube, such as blood vessels. We have theoretically demonstrated the dependence of the localized wave amplitude on the speed of the solitary pulse and on the nonlinear elasticity parameter. Explicit profiles for the localized excitations are presented. Furthermore, numerical simulations of the time-dependent

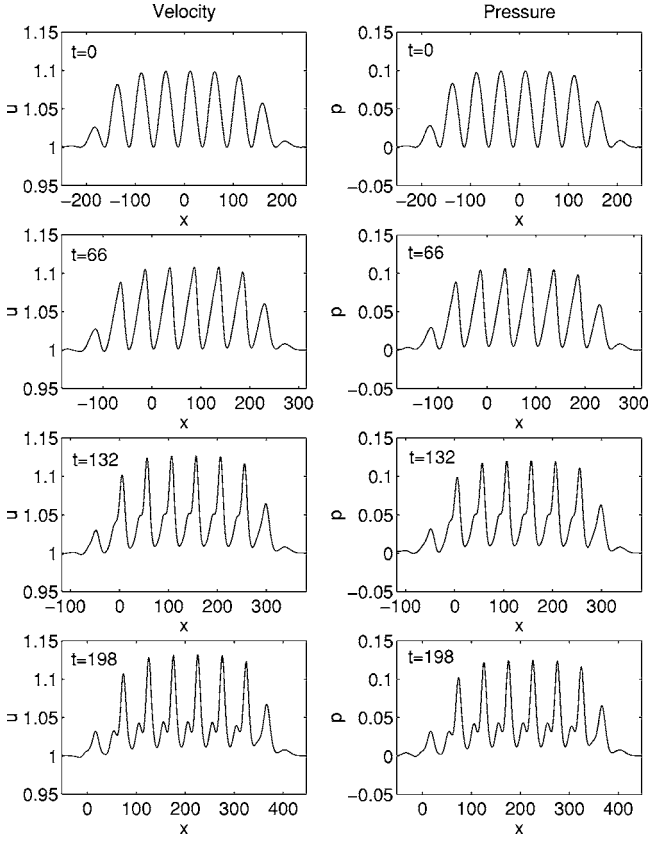

FIG. 3. The profile of the flow velocity (left panels) and pressure (right panel) at different times for $\alpha=2.0$.

nonlinear hydrodynamic equations reveal the formation of shock fronts and possible excitations of solitary pulses for a wide large-amplitude waves. We have also performed a numerical experiment with measured parameters from the thoracic aorta of a dog and could observe the formation of narrow dicrotic pressure pulses similar to the ones observed [1,2] in the ascending aorta to the saphenous artery. We stress that the nonlinear model used here is only valid for blood vessels with a large diameter ($\sim$1.5 cm) so that the viscosity of the blood can be neglected, while the viscosity should be included to extend the theory to blood vessels with smaller diameters.

ACKNOWLEDGMENT

This work was partially supported by the Deutsche Forschungsgemeinschaft through the Sonderforschungsbereich 591.

[1] D. A. McDonald, *Blood Flow in Arteries*, 2nd ed. (Edward Arnold, London, 1974).
[2] S. Yomosa, J. Phys. Soc. Jpn. **56**, 506 (1987).
[3] A. Sakanishi, M. Hasegawa, and Y. Ushiyama, Phys. Lett. A **221**, 395 (1996).
[4] Y. Hashimuze, J. Phys. Soc. Jpn. **54**, 3305 (1985).
[5] Y. Hashimuze, J. Phys. Soc. Jpn. **57**, 4160 (1988).
[6] J. F. Paquerot and S. G. Lambrakos, Phys. Rev. E **49**, 3432 (1994).
[7] J. F. Paquerot and M. Remoissenet, Phys. Lett. A **194**, 77

(1994).
[8] W.-S. Duan, B.-R. Wang, and R.-J. Wei, Phys. Rev. E **55**, 1773 (1997).
[9] H. Demiray, Int. J. Eng. Sci. **42**, 203 (2004).
[10] W. Malfliet and I. Ndayirinde, Physica D **123**, 92 (1998).
[11] S. Noubissie and P. Woafo, Phys. Rev. E **67**, 041911 (2003).
[12] J.-K. Xue, Phys. Lett. A **331**, 409 (2004).
[13] R. Z. Sagdeev, in *Reviews of Plasma Physics*, edited by M. A. Leontovich (Consultants Bureau, New York, 1966).
[14] R. Z. Sagdeev, Rev. Mod. Phys. **51**, 11 (1979).